

RESEARCH ARTICLE

Integration of an IEEE 802.15.4 RFID network with mobile readers with a 802.11 WLAN

Haleh Khojasteh, Jelena Mišić and Vojislav B. Mišić*

Ryerson University, Toronto, ON, Canada

ABSTRACT

In this paper, we propose a coexistence scheme that allows radio-frequency identification readers or sinks to collect data from radio-frequency identification tags or sensors that use IEEE 802.15.4 wireless personal area network standard and send it to the access point via an IEEE 802.11 wireless local area network. The proposed scheme uses time scheduling and bridging via readers to allow for simultaneous operation of heterogeneous wireless networks that operate in the industrial, scientific, and medical frequency band at 2.4 GHz. A simple sleep management approach is developed that allows tags to reduce their power consumption as well as collision rate. To provide timely reaction to sudden changes in tag population or reader availability, we devise a scheme where the scheduling parameters are adjustable and readers are mobile. We evaluate the performance of our solution in four scenarios and confirm the flexibility of the proposed approach. Copyright © 2012 John Wiley & Sons, Ltd.

KEYWORDS

RFID networks; wireless sensor networks; IEEE 802.15.4; IEEE 802.11; coexistence in the ISM band

*Correspondence

Vojislav B. Mišić, Ryerson University, Toronto, ON, Canada.

E-mail: vmisic@ryerson.ca

1. INTRODUCTION

Radio-frequency identification (RFID) is widely used in many industrial applications; quite a few of which rely on the use of active tags equipped with IEEE 802.15.4 low rate wireless personal area network (WPAN) interface [1,2]. However, transmitting RFID data to the respective data centers necessitates a multihop approach over heterogeneous wireless networks because of the comparatively short transmission range of 802.15.4 devices [3]. Multihopping may be achieved by enabling RFID readers to act as bridges by equipping them with two wireless interfaces: an 802.15.4 one to connect to the tags and another one to connect to an access point (AP) and, ultimately, to the server(s). A viable candidate for the latter hop is the ubiquitous IEEE 802.11 wireless local area network (WLAN) technology, which is cheap and readily available. However, both 802.15.4 and 802.11 operate in the same band—the unlicensed industrial, scientific, and medical (ISM) band at 2.4 GHz—which raises the issue of coexistence between these two network technologies [3,4]. Coexistence may be achieved through channel planning or by judicious scheduling of transmissions in both networks,

with the goal of minimizing, or even altogether eliminating, the probability of interference between them.

In this paper, we propose a time-division scheme for 802.15.4 and 802.11 networks operating in the ISM band; these networks will hereafter be referred as WPAN and WLAN, respectively. Coexistence is based on interleaved scheduling between the two networks that uses the slotted beacon-enabled carrier sense multiple access/collision avoidance (CSMA/CA) in the WPAN [1,5] and hybrid coordination function (HCF)-controlled channel access mechanism (HCCA) in the WLAN [6]. We describe the scheme, discuss the choice of parameter values, and evaluate its performance in different scenarios. As the cell space may include a large number of tags, keeping all tags active at all times would quickly deplete their energy sources. Therefore, we propose a sleep management scheme that keeps only a portion of available tags active at any given time and schedules their activity periods so as to minimize the probability of collisions between transmissions of tags in the same cell.

In the simplest case, the scheduling parameters are initially set and do not change afterwards, and the readers are stationary. However, many industrial scenarios include

abrupt changes in tag population (e.g., when a number of packaging container with many RFID tags arrive to the warehouse or leave it) or reader failures because of mechanical or electrical problems; neither of which can be handled with the stationary approach. To this end, we propose dynamic scheduling at the media access control (MAC) layer that is accomplished through adjustment of scheduling parameters and/or reader mobility; both of which are controlled by the AP.

The paper is organized as follows: Section 2 reviews current state of the art in this area. Section 3 provides the necessary background about IEEE 802.15.4 and IEEE 802.11 standards, and about HCCA and distributed coordination function (DCF) in particular, whereas Section 4 presents our coexistence scheme, together with sleep management, in detail. Section 5 presents initial performance evaluation of the scheme under stationary conditions. Amendments related to dynamic scheduling are discussed and evaluated in Section 6. Finally, Section 7 concludes the paper and highlights some avenues for future research.

2. RELATED WORK

Related work at the MAC and network layers mostly comes from the area of wireless sensor networks, where issues such as interference and coexistence, multihopping, energy management, and dynamic scheduling of cluster head nodes were addressed by many researchers.

From the aspect of coexistence at physical layer, [7] has demonstrated that deployment of IEEE 802.11 and IEEE 802.15.4 in overlapping frequency band results in packet losses for IEEE 802.15.4 depending on degree of spatial and frequency separation. The problem is even more difficult because in IEEE 802.15.4, only channel 26 is free of interference from nearby IEEE 802.11 networks (Figure 1).

Regarding routing, the main question is whether single hopping is possible in view of transmission range and power limitations, or multihopping must be used. While the latter solution allows the area covered by the network to exceed the transmission range of individual nodes, it also makes energy management more complicated because bridge or relay nodes will consume power at a much faster rate than ordinary sensor nodes. The introduction of mobility—for the base station/sink, cluster head nodes, or even all nodes—further complicates the problem.

One of the most popular protocols to address these problems is low-energy adaptive clustering hierarchy (LEACH) [8], which includes distributed cluster formation, local processing to reduce global communication, and randomized rotation of the cluster heads, which allows it to achieve balanced power consumption among all nodes. Among the many extensions of LEACH, [9] proposes a routing protocol for mobile nodes called 2L-LEACH-M where the nodes are subdivided into two levels to facilitate the selection and rotation of cluster heads.

Much research effort has been devoted to finding the best path for data transmission from nodes to cluster heads. Some authors [10,11] analyzed routing by simply considering the number of hops from node to the cluster head or to the base station/sink. A number of authors [12–14] have discussed the case where the base station (i.e., network sink) was mobile. In this scenario, the cluster head registers the tree-like backbone structure on behalf of the sink, and then the sensor nodes were sending their data to the respective cluster heads via that tree. A different approach was discussed in [15], where both sensor nodes and cluster heads were mobile, whereas the base station/sink was static and, moreover, always aware of cluster heads' position. In [16], all nodes were mobile, and each cluster contains one acting cluster head and two deputy cluster head nodes.

Cluster head mobility was also investigated in a number of papers. In [17,18], a few energy-rich nodes were designated as cluster heads that move in a controlled manner toward locations that were rich in energy and data, with the goal of distributing the remaining energy evenly in the network. In addition, the cluster heads tried to maintain a connected path to the base station. The work in [19,20] sought to determine the location of the mobile base station that would ensure energy-efficient data delivery through cluster heads. Dynamic positioning of mobile cluster heads was found to be an NP-hard problem, and an efficient heuristic was proposed as a substitute [21].

A distributed clustering algorithm was proposed on the basis of multicriterion metric combining connectivity, coverage, mobility, and residual energy [22]. Another protocol was defined to find the most suitable cluster head, perform data fusion, and find the most trusted neighbors for sending the fusion result to base station in [23]. In [24], a three-layer framework was proposed for mobile data collection in wireless sensor networks, which included the sensor layer, cluster head layer, and mobile collector

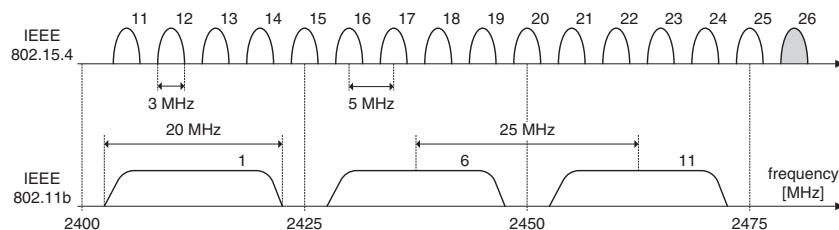


Figure 1. Channel assignment of IEEE 802.11 and IEEE 802.15.4 standards in the industrial, scientific, and medical band.

(called SenCar) layer. At the mobile collector layer, the SenCar was equipped with two antennas, which enabled multiple cluster heads to simultaneously upload data to the SenCar. The trajectory planning for the SenCar was optimized to fully utilize MIMO uploading capability by selecting polling points in each cluster. By visiting each selected polling point, the SenCar could gather data from cluster heads and transport the data to the static data sink.

An interesting variation on this theme is the clustering-based multichannel MAC protocol designed for vehicular ad hoc networks in [25]. In this scheme, one vehicle was selected as a cluster head, and a dynamic channel assignment was used to solve the collision problem and increase network throughput. In [26], an algorithm based on the synchronized and shared contention window concept of IEEE 802.11 DCF was defined for a mobile wireless sensor network and the optimum value of the contention window that results in minimum energy cost for a given number of nodes in a cluster. Furthermore, in [27], a mechanism was defined to balance the static cluster head's load on the basis of the distribution of mobile sensor nodes in IEEE 802.15.4 protocol.

In [28], a wide area indoor location system was proposed that determines three-dimensional location for a target object by using triangulation method and the Kalman filter. The algorithm is lightweight and was deployed in ZigBee-based network, but impact of MAC layer was not explicitly addressed.

The main difference between the models mentioned earlier and our solution described in the following lies in the explicit combination of MAC and physical layers of IEEE 802.11e and 802.15.4 protocols, which the other models do not utilize; in addition, our solution deploys a randomized sleeping technique for tags to decrease collisions.

3. BACKGROUND: IEEE 802.15.4 AND 802.11 STANDARDS

The main obstacle to coexistence of IEEE 802.14 and IEEE 802.15.4 stems from the fact that channels assigned to WPAN compliant with the IEEE 802.15.4 standard overlap with those assigned to WLAN compliant with the IEEE 802.11 standard, as shown in Figure 1. As WLAN nodes have wider channels and use one or two orders of magnitude higher transmission power than WPAN nodes, interference will lead to degradation of WPAN performance, and simultaneous operation of the two networks is virtually impossible. Moreover, ISM band is license-free,

and new WLAN networks can appear at any time and at any channel. Consequently, channel/frequency planning cannot be used, and any coexistence scheme must be based on careful scheduling of WLAN and WPAN operations. With this notion, we will now briefly review the operation of IEEE 802.11 and IEEE 802.15.4 standards, with particular emphasis on features that are similar but implemented in a different way in the two.

3.1. IEEE 802.11 and its HCCA mechanism

Most IEEE 802.11 WLANs use the contention-based channel mechanisms known as DCF or enhanced distributed channel access (EDCA) [6]; in both of which, nodes attempt medium access after a random backoff period during which the medium is free. In addition, EDCA allows traffic to be prioritized through differentiation of contention window interframe space and duration of transmission opportunity. Still, this approach is not well suited for real-time traffic, which is better served through HCCA, typically used to achieve quality of service (QoS) for real-time multimedia services or to improve energy efficiency.

The HCF is composed of two access methods: contention-based channel access through EDCA and controlled channel access through HCCA. HCCA can start the controlled channel access mechanism in both contention-free period (CFP) and contention period (CP) intervals. During the CP, a new contention-free subperiod named controlled access phase (CAP) is introduced, in which frames are transmitted using HCCA. HCCA can start a CAP by sending downlink QoS frames or QoS CP-poll frames to allocate polled transmission opportunity to different QSTAs after the medium remains idle for at least point coordination function interframe space interval; the remaining time of the CP can be used by EDCA. This contention-free scheme is fairly flexible, which is why CFP is made optional in the 802.11e standard [29].

Figure 2 shows a typical 802.11e beacon interval (BI). At the beginning of each cycle, AP broadcasts a beacon frame with information about the durations of CFP and CP and the total duration of the cycle. During the CFP, the AP will poll one of the nodes, and the node will reply with acknowledgement. After that, the medium is dedicated to the polled node until the end of CFP period. Throughout the CFP period, other nodes will wait without attempting to transmit. During the CP, nodes compete with each other to access the medium by using the EDCA or DCF mechanism. If CAP intervals are defined during the CP, the system will be in the polling mode.

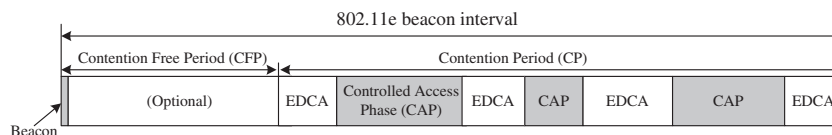


Figure 2. A typical 802.11e hybrid coordination function beacon interval (adapted from [6]).

Table I. Timing parameters in the WLAN network.

Parameter	Label	Value
Basic time slot	σ_1	20 μ s
Time unit	T_1	1024 μ s
SIFS		10 μ s (0.5 σ_1)
PIFS		30 μ s (1.5 σ_1)
DIFS		50 μ s (2.5 σ_1)
Basic data rate		2 Mbps
Beacon size		2 σ_1
Polling frame		14 σ_1
Polling ACK frame		14 σ_1
CF-END frame		14 σ_1
RTS frame		14 σ_1
CTS frame		13 σ_1
DCF ACK frame		13 σ_1
Contention window	minCW ₁	32
(in basic slots)	maxCW ₁	1024

WLAN, wireless local area network; SIFS, short interframe space; PIFS, interframe space interframe space; DIFS, DCF interframe space; ACK, acknowledgement packet; CF-END, end of the contention-free period (CFP); RTS, request to send; CTS, clear to send; DCF, distributed coordination function.

Table I presents default values of WLAN timing parameters, denoted with subscript ‘l’ to distinguish them from their WPAN counterparts, where subscript ‘p’ will be used.

In this paper, during the WLAN active periods of CP, plain DCF is used, with CSMA/CA as the basic mechanism for medium access. A node that wants to transmit a packet must listen to the channel to make sure no other node is transmitting, and transmission can be undertaken only if the channel is clear during a randomly chosen time interval (backoff time). The backoff time is uniformly chosen in the range (0, CW – 1), where CW is the current size of the contention window that may range from minCW₁ to maxCW₁, as per Table I. Backoff counter will be decremented after each slot time if the transmission medium is free; otherwise, its value will be frozen until the medium becomes free again for DCF interframe space time units (slot time is derived from the propagation delay time to switch from receiving to transmitting mode and time to pass the information about the physical channel state to MAC layer). Station will transmit when its backoff counter reaches zero.

When the packet is received, receiver replies with an acknowledgement packet after short interframe space time interval. Whenever packet collision occurs, acknowledgement will not be received within short interframe

space + acknowledgement packet time, and transmission has to be reattempted with the contention window doubled in size (but not exceeding maxCW₁). To limit packet collision time and guard against hidden terminal problem, the standard provides a three-way handshake mechanism that uses request to send and clear to send packets, sent using CSMA/CA prior to actual packet transmission [6].

3.2. Basic properties of IEEE 802.15.4 MAC

The coexistence scheme is based on interleaved scheduling, which necessitates the presence of cycles or superframes. IEEE 802.15.4 standard allows such operation mode, known as slotted, beacon-enabled mode of operation, with one WPAN coordinator and many ordinary nodes [1]. Each superframe begins with the transmission of a beacon frame, followed by an active portion (in which data transmission takes place) and an optional inactive portion (in which nodes can sleep), as shown in Figure 3. The raw data rate for operation in the ISM band is 250 kbps, and the basic time unit is one backoff period of 10 bytes. Duration of the active superframe part is denoted as superframe duration (SD), whereas the duration of the entire superframe (i.e., the time interval between two successive beacon frames) is referred to as the BI. These durations in backoff periods are determined by the MAC variables superframe order (SO) and beacon order (BO) so that $SD = 48 \cdot 2^{SO}$ and $BI = 48 \cdot 2^{BO}$, expressed in unit backoff periods, where $0 \leq SO \leq BO \leq 15$.

An active superframe part consists of a contention-based part and an optional guaranteed time slot part. During the contention-based part, a node that wants to transmit a packet has to perform a random backoff (during which it does not listen to the medium, unlike its WLAN counterpart) and then listen to the channel during two unit backoff periods (clear channel assessment periods). If the channel is idle, the node can transmit the packet and, if requested, receive an acknowledgement from the destination. As in a WLAN, the backoff value is uniformly chosen in the range from 0 to CW₁, the current contention window. Furthermore, if the active portion of the superframe ends while a countdown is in progress, the countdown will be frozen during the inactive portion of the superframe and will resume immediately after the beacon in the next superframe. Also, if a countdown ends but the remaining time in the superframe does not suffice for two clear channel

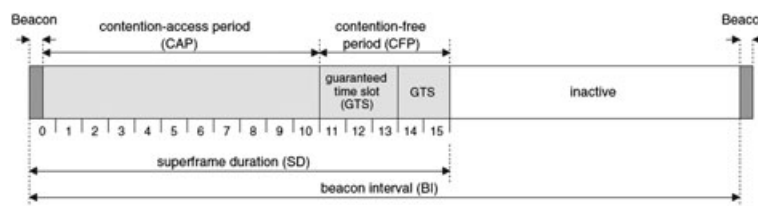
**Figure 3.** The composition of the superframe under IEEE 802.15.4 (adopted from [1]).

Table II. Timing parameters in the WPAN.

Parameter	Label	Value
Unit time slot	σ_p	320 μ s
Beacon size	$2\sigma_p$	
Raw data rate		250 kbps
Contention window (in unit slots)	$CW_{15_{min}}$	7
	$CW_{15_{max}}$	31

WPAN, wireless personal area network.

assessments, packet transmission, and optional acknowledgement, all of those activities are deferred to the next superframe [1].

Table II illustrates the timing parameters of IEEE 802.15.4 that we are using in our design.

4. BRIDGING AND SCHEDULING BETWEEN WLAN AND IEEE 802.15.4

Let us now consider the coexistence scheme, using an example topology, shown in Figure 4, which consists of a WLAN with an AP and two WPAN cells. The coexistence problem is solved by time-division multiple access—time sharing between the WPAN (i.e., reader(s) and tags) and WLAN (i.e., the AP and readers communicating through their IEEE 802.11 interface). Readers participate in both networks and thus provide the bridging function between the two networks. Because of the different channel allocation, as shown in Figure 1, a single AP and its WLAN can support multiple WPAN cells that may use different WPAN channels.

In this topology, the AP will periodically broadcast beacon frames with information about the duration of timing

periods. This information will then be used by the readers to schedule the WPAN superframes, as illustrated in Figure 5.

Each cycle starts with a beacon frame sent from the AP; this beacon includes the length of cycle. In our model, we only use the CP of HCF mechanism as the CFP is optional according to Section 3.1. The CP is divided into four sub-cycles that are equal in time length. The reason we have considered four subcycles (instead of three subcycles) is the timing calculations at RFID networks' side. The first subcycle is completely dedicated to WLAN devices' activity, but the second, third, and fourth subcycles have a CAP interval at the beginning that is dedicated to the RFID networks' activity, and then the second part of the subcycle is given to WLAN network. The AP polls the prospective readers, one per CAP period, in round robin order. The polled reader will send an acknowledge frame to AP and then send a beacon signal to its cell (i.e., WPAN), thus initiating a new active portion of the superframe in its cell. The active tags in this cell region will try to send their data by using the CSMA/CA algorithm of IEEE 802.15.4 standard.

During the CAP period, other readers and other WLAN devices, if any, are waiting. This allows the tags in the WPAN cell to work without interference. They try to send their information to the reader, which will aggregate the data and create new data packet(s) to send to the AP.

At the end of CAP period, the active reader will send a CF-END frame to AP to announce the end of its activity. During the ensuing contention-based WLAN active period, the reader switches to its 802.11 interface and attempts to send the aggregated tag data to the AP, competing with the medium with other readers and WLAN devices. As it was mentioned in Section 3.1, The WLAN devices and RFID

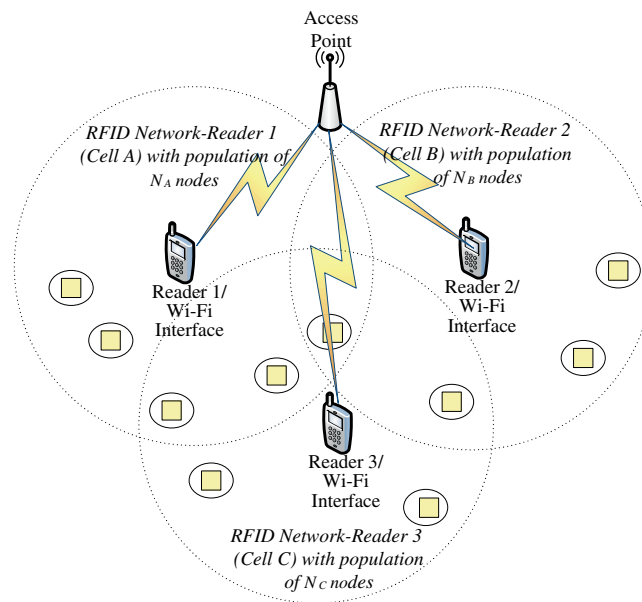


Figure 4. Proposed topology.

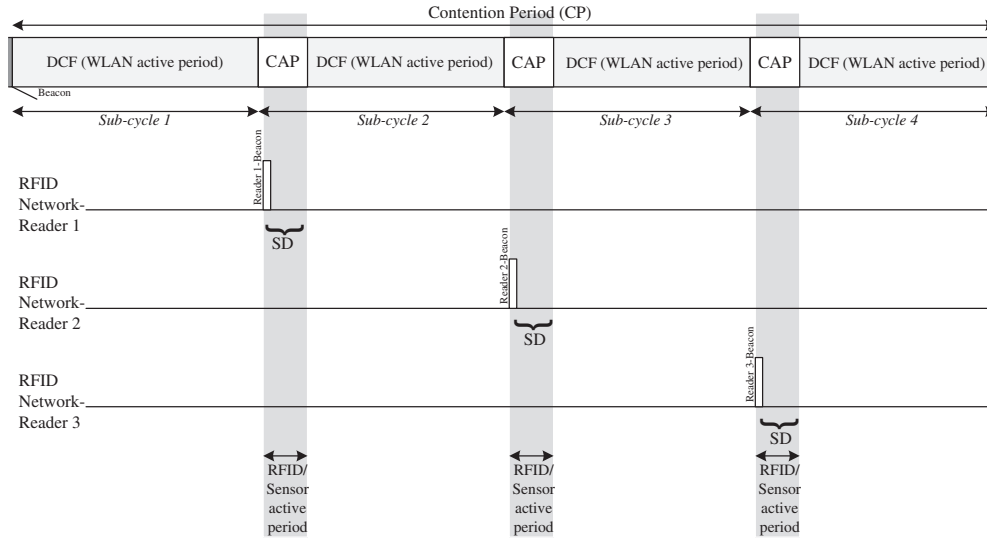


Figure 5. Timing of access point time scheduling.

readers are using DCF mechanism for their communication with AP.

Another WLAN cycle then begins with another beacon sent from the AP.

In this manner, the AP polls the readers and allows their respective WPANs to operate in a round robin scheme.

4.1. Superframe timing parameters

Table III shows typical values of the timing parameters used in our design.

The minimum duration of the active portion of WPAN superframe is 15.36 ms or 480 bytes, which corresponds to SO of $SO = 0$. As the size of WLAN subcycle is chosen approximately $100T_1$ and the WPAN BI is about four times that value, as per Table III, then $BO \approx 4.7$, which can be rounded to 5. In this case, $BI = 2^5 \cdot 15.36 \text{ ms} = 491.52 \text{ ms}$, which is the chosen WPAN BI whereas the WLAN cycle is $= 4 \cdot 8 \cdot 48 \cdot 16 \cdot \sigma_1 = 24576 \cdot \sigma_1$.

The total size of the data frame (with headers) for WPAN tags is 30 bytes. Thus, we have $30 \cdot 8/250 \text{ kbps} = 0.96 \text{ ms}$ and $0.96 \text{ ms}/0.320 \text{ ms} = 3 \sigma_p$ for the total duration of data frame.

Table III. Calculated timing parameters.

Data frame size	30 bytes (σ_p)
WLAN superframe	491.52 ms ($24576\sigma_1$)
WLAN subcycle	122.88 ms ($6144\sigma_1$)
WPAN superframe (BI)	491.52 ms ($1536\sigma_p$)

WLAN, wireless local area network; BI, beacon interval.

4.2. Calculation of sleeping probability

To reduce energy consumption and avoid collisions to the largest extent possible, most RFID tags are sleeping. They wake up asynchronously with each other and wait until they hear a WPAN beacon frame, which indicates that the reader is ready to receive the data from the tags. Tags use CSMA/CA mechanism in accordance with the 802.15.4 standard; if the transmission is successful (i.e., once they receive an acknowledgment from the reader), they can go back to sleep.

Obviously, the longer tags sleep, the smaller the number of active tags at any given time and the probability of collision among them will decrease. Later in Section 6, we will discuss the way in which this effect can be countered.

The sleep period is calculated as a random value from a given distribution with a given mean, similar to the randomized scheme described in [30]. If the probability distribution of sleep time (in time slots) is described with a probability generating function [5] of

$$T_{\text{sleep}}(z) = \sum_{k=1}^{\infty} p_k z^k, \quad T_{\text{sleep}}(1) = 1$$

the average sleep time is $\overline{T_{\text{sleep}}} = \sum_{k=1}^{\infty} k \cdot p_k = T'_{\text{sleep}}(1)$.

If the distribution of sleep time is geometric, then we have

$$\begin{aligned} T_{\text{sleep}}(z) &= \sum_{k=1}^{\infty} (1 - P_{\text{sleep}}) P_{\text{sleep}}^{k-1} \cdot z^k \\ &= \frac{(1 - P_{\text{sleep}})z}{1 - zP_{\text{sleep}}} \end{aligned}$$

Table IV. Sleeping parameters for clusters.

Average sleep time		Sleep probability (P_{sleep})
Hours/minutes	Time slots	
1 min	115207.3733	0.9999913200
2 min	230414.7465	0.9999956600
5 min	576036.8864	0.9999982640
10 min	1152073.733	0.9999991320
15 min	2812500	0.9999996444444
30 min	5925000	0.9999998222222
1 h	11250000	0.9999999111111
1.5 h	16875000	0.9999999407407
2 h	22500000	0.9999999555555

and $\overline{T_{\text{sleep}}} = T'_{\text{sleep}}(1) = \frac{1}{1 - P_{\text{sleep}}}$. We can now calculate P_{sleep} for a given average sleep time in seconds (X_s) as

$$\frac{X_s}{0.00032} = \frac{1}{1 - P_{\text{sleep}}}$$

In this equation, 0.00032 is the size of each IEEE 802.15.4 unit backoff period in seconds. Once P_{sleep} is known, every sleep period will be calculated as a random variable.

We have calculated P_{sleep} for different average sleep times; as shown in Table IV, average sleep time in minutes

or hours and in time slots and also their corresponding sleep probability are presented.

5. PERFORMANCE EVALUATION

To evaluate the performance of the proposed approach, we have built a discrete event simulator of a two-tier network with two WPAN cells and one AP-based WLAN network, using object-oriented Petri net-based simulation engine Artifex by RSoftDesign, Inc. [31]. In the simplest case, readers are stationary, whereas the tag population is constant. In static topology, the readers are stationary. Moreover, the scheduling of IEEE 802.15.4 is static; SD size is constant, and it is equal to 480 bytes, which is the minimum size defined in IEEE 802.15.4 standard. In this approach, the average sleep time (X_s) and number of tags in each cell (N_A, N_B, N_C) change in different scenarios, and the effects of these changes on the system are tested.

In Scenario 1, we have one WLAN with an AP, and three WPAN cells with the corresponding readers/bridges as in Figure 4. The readers are stationary, WPAN parameters are fixed, and the average sleep time (X_s) is constant (1 min), but the number of tags in each cell (N_A, N_B, N_C) is variable. The performance of the

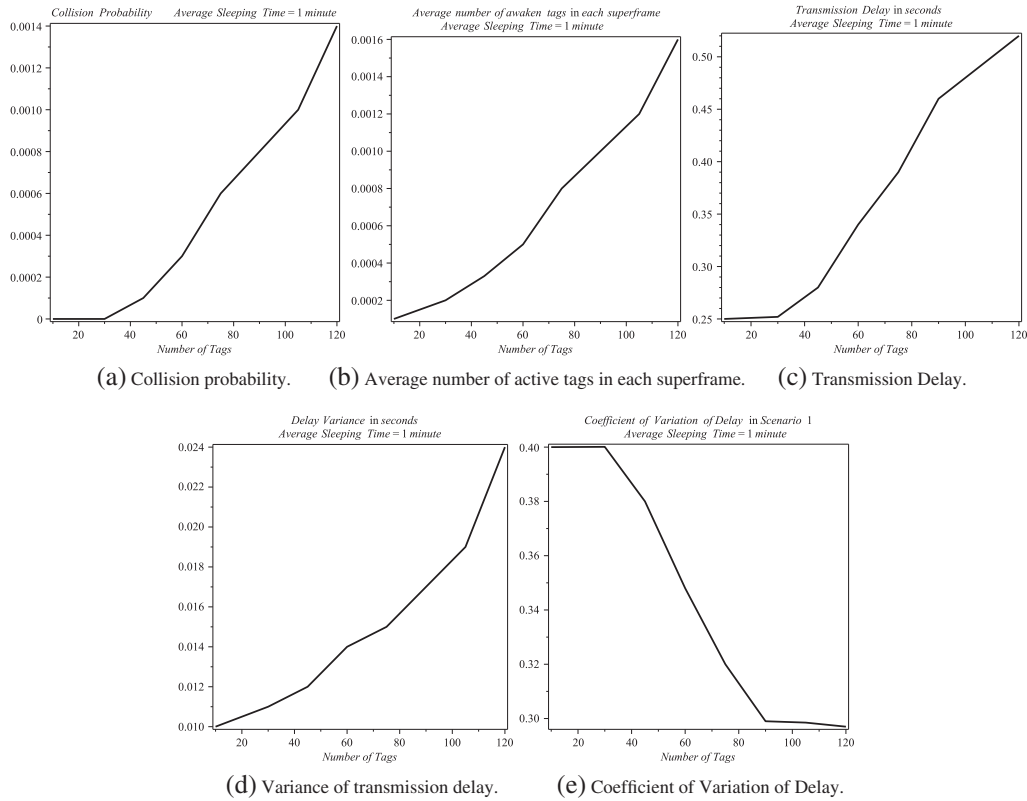


Figure 6. Simulation results of Scenario 1: variable number of tags in each radio-frequency identification network and constant average sleep time (1 min). (a) Collision probability, (b) average number of active tags in each superframe, (c) transmission delay, (d) variance of transmission delay, and (e) coefficient of variation of delay.

coexistence scheme is evaluated through the evaluation of the packet collision probability.

As can be seen in Figure 6(a), virtually no collisions are detected if the number of tags per cell is below 30. The collision rate increases when the number of tags in each cell is increasing; the collision probability for 120 tags in each cell is about 0.14%, which is still acceptable. Figure 6(b) shows the number of active tags in each superframe which, as expected, increases when the total number of tags per cell increases. Moreover, in this scenario, with increasing number of tags in each cell, transmission delay increases according to Figure 6(c). This matches the assumption that more crowded cells face more delay in their transmissions. Furthermore, delay variance increases when the number of tags in the cell increases, as shown in Figure 6(d), but because the average delay increases at an even faster rate, the coefficient of variation of delay actually decreases, as can be seen in Figure 6(e). Also, the transition from linear to saturation regime can be observed clearly.

In Scenario 2, we set the number of tags in each cell to 90 but vary the average sleep time; all other parameters are the same as in the previous experiment.

According to Figure 7(a), increasing the average sleep time in each cell leads to decreasing collision rate. Moreover, the collision probability for 1 min average sleep

time (which is the worst case in our tested cases) is only about 0.08%, with virtually zero collisions detected for average sleep times in excess of 10 min. The average number of active tags decreases when the average sleep time increases, as shown in Figure 7(b). Furthermore, with increased sleep time in each cell, transmission delay decreases, as shown in Figure 7(c). The results show that if the tags sleep longer, there will be fewer active tags and fewer collisions, which means transmission delays will be shorter. Moreover, delay variance decreases according to Figure 7(d). These results confirm that if tags are sleeping more, we will get closer to the average value of transmission delay. The coefficient of variation of delay has been shown in Figure 7(e); the increase of average sleeping time leads to fewer collisions and drives the network away from saturation.

To further evaluate the effect of average sleeping time of RFID tags on the collision probability, we have also investigated the impact of the average tag sleeping time. Figure 8 shows that, after decreasing the average sleeping time beyond approximately 40–50 s, collision probability indicates that the network has reached linear operating regime.

On the other hand, changing the size of CAP or DCF does not have a significant effect on the tag collision rate

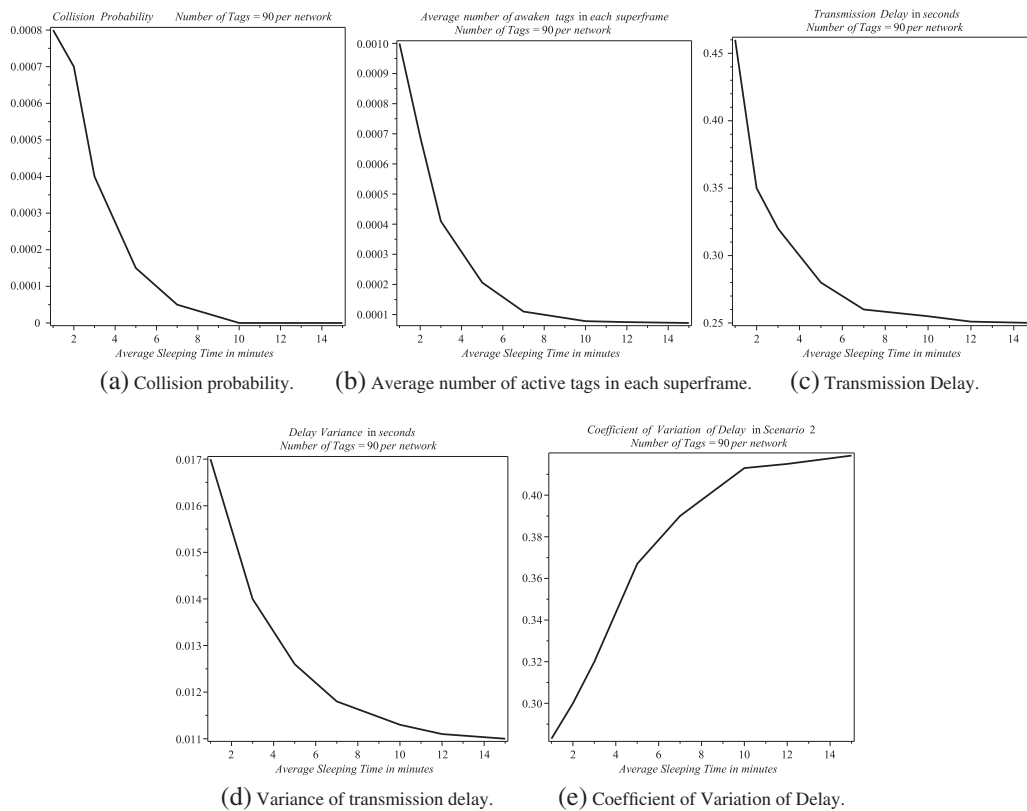


Figure 7. Simulation results for Scenario 2: variable average sleep time and constant number of tags in each radio-frequency identification network (90 tags). (a) Collision probability, (b) average number of active tags in each superframe, (c) transmission delay, (d) variance of transmission delay, and (e) coefficient of variation of delay.

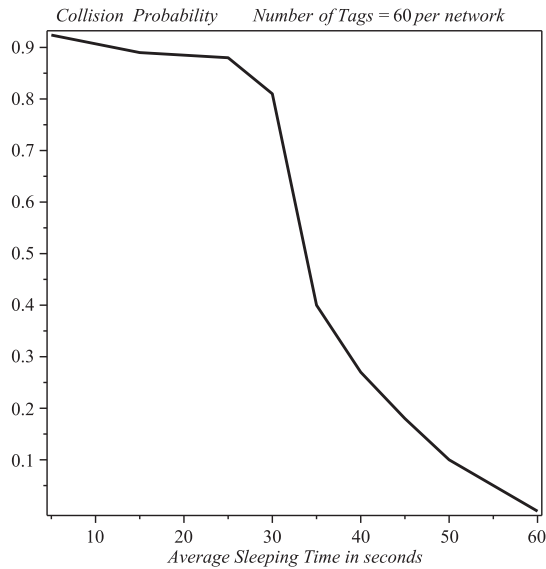


Figure 8. Collision probability in case of changing the average tag sleeping time.

and, thus, will not resolve the collision problem. The length of a WLAN subcycle is approximately 100 ms, and we have used the closest value, which is a power of two of multiple of 32 ms time slot on the RFID side. According to Figure 8, sleeping time of nodes has a major effect on collision rate, and if the average sleeping period of nodes becomes progressively smaller, collision probability of nodes increases, and with smaller average sleeping periods, saturation will occur. As the result, changing the size of superframe cannot resolve this issue.

6. THE DYNAMIC APPROACH

The approach presented earlier can easily handle scenarios in which the numbers of tags and readers in a cell are stationary; it is thus applicable to many wireless sensor network applications. However, in industrial RFID scenarios, abrupt changes in tag population or reader functionality are not uncommon. For example, the number of tags in a given cell may suddenly increase because of the arrival of a large shipment container with many tags or decrease because of a large number of packages being shipped out for transport or distribution. Also, a functioning reader may cease to operate due to a mechanical failure or battery exhaustion. In such cases, offline selection of parameters will result in insufficient performance or, in the worst case, in virtual failure of an entire cell. Therefore, a different approach is needed—the one in which scheduling parameters may be dynamically adjusted and the readers may move so as to cover the cells that need additional reader capacity. In this Section, we present some simple yet effective algorithms that will allow us to maintain the performance at a desired level.

6.1. SD size adjustment algorithm

As noted earlier, one possible cause of performance problems is an abrupt change in the population of tags in a single cell. In particular, an increase in the number of tags can lead to saturation: as many tags wake up and try to contact the reader, the collision rate will suddenly increase, and the transmission success rate will drop. To maintain the collision rate at an acceptable level and make the best use of SD period, we have defined an algorithm through which the AP will determine the size of SD, as shown in Algorithm 1.

Initially, the SD is set to the minimum value of 480 bytes. In each round, the algorithm reads data from active tags (i.e., those that are awake) and estimates the total number of tags in the cell. Because the number of tags can change abruptly, we have to use smoothing to control the effect of sudden changes on the system; to this end, we have used the exponentially weighted moving average technique. We use x_k to denote the new estimate of the total number of tags, x_{k-1} for the previous estimate and e_k for the number of tags contacted in the current read round. If the difference between the current and previous number of tags is greater than some predefined threshold ε , Algorithm 1 invokes Algorithm 2 to adjust the SD size.

Algorithm 1 Determine SD size.

- 1: Start with minimum SD size;
 - 2: **while true do**
 - 3: Perform a read round with active tags;
 - 4: Record the number of active tags as e_k ;
 - 5: Estimate the total number of tags as

$$x_k = (1 - \alpha)x_{k-1} + \alpha e_k;$$
 - 6: **if** ($|x_k - x_{k-1}| < \varepsilon$) **then**
 - 7: Adjust the SD size using Algorithm 2 and store it;
 - 8: **end if**
 - 9: Store the number of collided packets;
 - 10: Store the number of successful packets;
 - 11: Store the number of idle packets;
 - 12: **end while**
-

In Algorithm 2, we use a revised estimate for the number of tags: not the count of packets received successfully in the previous round (which is used as a proxy measure for the number of active tags) but the count of successful packets plus twice the count of collided packets because at least two tags are involved in a collision [32]. As before, we use exponential smoothing to estimate the total number of tags.

After finding the revised estimate, Algorithm 2 looks up the information in Table V to find the best size of SD. The bounds of optimum range overlap a little to produce a small hysteresis effect so as to avoid frequent changes in superframe size. Our SD size selection scheme is similar to the frame size selection presented in [32], but the boundaries and superframe sizes are selected according to the requirements of IEEE 802.15.4 standard. Note that the

Algorithm 2 SD size adjustment process.

- 1: Estimate the revised number of active tags as $f_k = S + 2C$;
- 2: Update the total number of tags as $x_k = (1 - \alpha)x_{k-1} + \alpha f_k$;
- 3: Use Table V to choose the appropriate SD size;
- 4: **if** ($x_k > 70$) **then**
- 5: Consider the cell as crowded and choose a new reader;
- 6: Move the reader to the cell using the algorithm from [28];
- 7: **end if**

Table V. SD size selection.

SD size (bytes)	Low	High
480	1	18
960	16	35
1920	32	70

SD, superframe duration.

superframe size must remain between 480 and 1920 bytes; if the number of tags is so high as to necessitate a longer superframe size, the AP concludes that the reader cannot handle all of the active tags in that cell and considers the cell to be crowded. In this case, the AP calculates the direction and distance for a specific reader from its current location (where it may or may not have been active at the current moment) toward the crowded cell by using the algorithm presented in [28] and instructs the reader to move to the specified cell.

We note that, because of the differences between test scenarios and evaluated parameters in [32] (such as weighted error and accuracy) and the ones in this paper, direct comparison of results is not possible.

To determine the impact of exponentially weighted moving average smoothing factor (α) in this scheme, we have performed an experiment where reader 1 becomes active after a long inactive period. As there are many active tags that try to send their IDs, there will be many collisions before the SD size increases, and high transmission success probability is reached. Three different values for α have been selected (0.1, 0.25, and 0.75), with a constant number of 60 active tags and the average sleeping time of 1 min. As can be seen in Figure 9, at the value of $\alpha = 0.75$, the cell will reach the high performance condition faster, but SD will also be more sensitive to small changes in tag population. On the other hand, when α is smaller (0.1), it takes more time to reach high transmission success probability. Consequently, we have chosen the value of $\alpha = 0.25$ as the best compromise.

6.2. Performance evaluation

To validate the proposed dynamic approach, we have tested two scenarios: in Scenario 3, the tag population is increased abruptly, and we add a new reader to cope with the

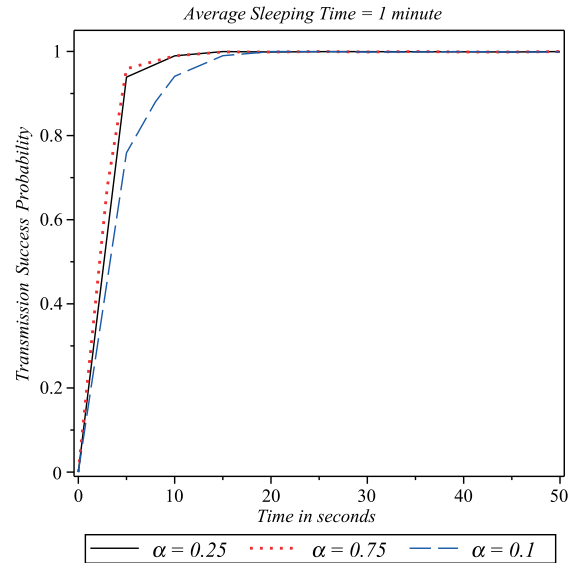


Figure 9. Effect of exponentially weighted moving average smoothing factor (α) on performance in cell A.

increase. In Scenario 4, the reader of one of the cells is broken after a while, and the system handles the situation by sending a new reader to that area. To measure the performance of our design, we have simulated our solution by using Artifex simulation environment.

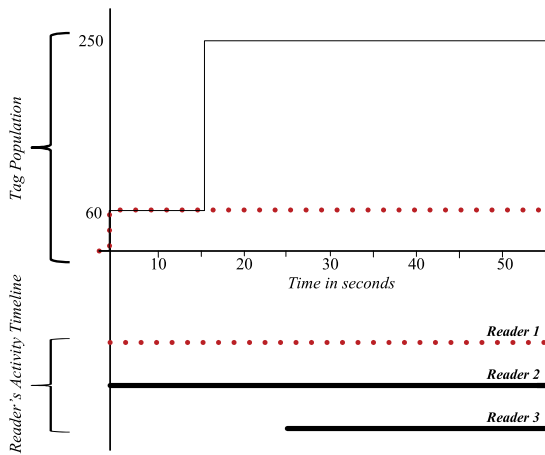
6.2.1. Scenario 3: abrupt change in tag population.

In this scenario, we have set up two test areas, cells A and B, with a total of three readers; the corresponding timing diagram is shown in Figure 10(a). In both cells, RFID tag population is set to 60 tags each in the beginning of the experiment. Initially, readers 1 and 2 are assigned to cells A and B, respectively, by the static scheduling algorithm, whereas reader 3 is inactive. As can be seen from Figure 10(b), the transmission success probability for tags in this cell stabilizes at the value close to 0.9997 after approximately 15 s (dotted line). Similar behavior can be seen in cell A, where the initial population of 60 tags is serviced by reader 2 (solid line).

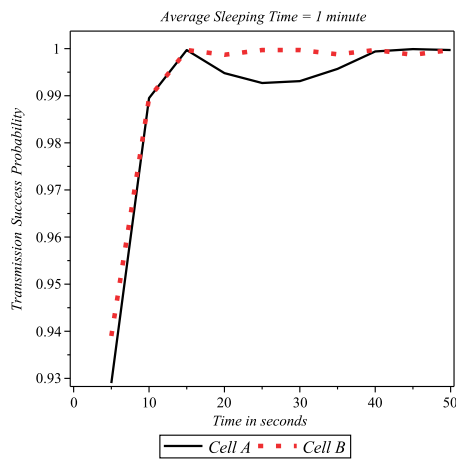
At 15 s, however, the population in cell A abruptly increases to 250 tags, which causes the transmission success probability to drop to a value close to 0.99; as the result, at about 25 s from the beginning of the experiment, a new reader (3) is assigned to this cell as per Algorithm 3. Transmission success probability then recovers, and it soon reaches a stable value close to the original one (0.9997).

6.2.2. Scenario 4: reader failure.

This scenario also begins with two cells, A and B, with 60 tags and one reader (1 and 2, respectively) in each of them; the corresponding timing diagram is shown in Figure 11(a). As before, the transmission success probability stabilizes at about 0.9997 after about 15 s



(a) Population of tags and reader activity.



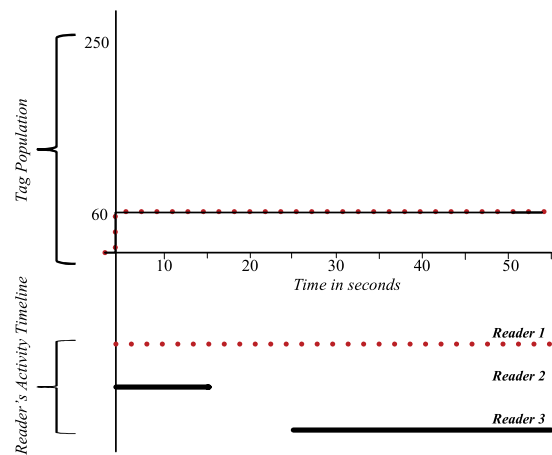
(b) Transmission success probability.

Figure 10. Scenario 3: abrupt change in tag population, allocation of a new reader. (a) Population of tags and reader activity and (b) transmission success probability.

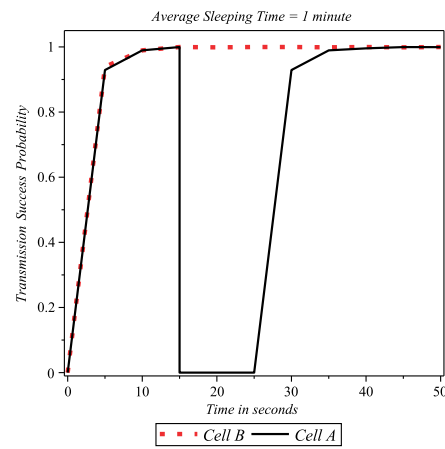
into the experiment. However, at 15 s, reader 2 ceases to operate, and transmission success probability in cell A (solid black line) immediately drops to zero, as shown in Figure 11(b). Algorithm 3 is again invoked, and it reassigns a mobile reader 3 that arrives to the cell at 25 s. Transmission probability begins to rise almost immediately; it exceed 0.9 after only about 5 s and reaches its stable value of 0.9997 after about 15 s (i.e., around 40 s into the experiment).

7. CONCLUSION AND FUTURE WORK

In this paper, we have proposed a time scheduling solution for the WLAN/RFID coexistence problem in ISM frequency band. By combining a time scheduling solution with a sleep management scheme for RFID tags, we have reduced the energy consumption, collision rate, and



(a) Population of tags and reader activity.



(b) Transmission success probability.

Figure 11. Scenario 4: reader failure of a reader, allocation of a new (mobile) reader. (a) Population of tags and reader activity and (b) transmission success probability.

transmission delay. Although the performance of the simplest approach in which scheduling parameters are defined beforehand is sufficient for wireless sensor network applications, it is not well suited for industrial RFID applications where the numbers of tags and readers are not stationary, and dynamic scheduling of tags as well as the availability of mobile readers is considered. Our results indicate that the scheme thus improved may support large variations in tag population as well as provide rapid reaction to reader failures.

In our future work, we will use the model presented in this paper as the underlay of a multiclustering model and test the routing issues among the clusters.

ACKNOWLEDGEMENT

This research is partly supported by the NSERC Discovery Grant.

REFERENCES

1. IEEE. *Wireless MAC and PHY Specifications for Low Rate WPAN. IEEE Std 802.15.4*. IEEE: New York, NY, 2006.
2. Gutiérrez JA, Callaway Jr. EH, Barrett Jr. RL. *Low-Rate Wireless Personal Area Networks*. IEEE Press: New York, NY, 2004.
3. Zhang L, Wang Z. Integration of RFID into wireless sensor networks: architectures, opportunities and challenging problems. In *Proceedings of Fifth International Conference on Grid and Cooperative Computing Workshops (GCCW'06)*, Maui, HI, October 2006; 463–469.
4. Mišić J, Mišić VB. Bridging between IEEE 802.15.4 and IEEE 802.11b networks for multiparameter health-care sensing. *IEEE Journal on Selected Areas in Communications* 2009; **27**(4): 435–449.
5. Mišić J, Mišić VB. *Wireless Personal Area Networks: Performance and Interconnections and Security with IEEE 802.15.4*. John Wiley & Sons: Chichester, UK, 2008.
6. IEEE. *Wireless LAN MAC and PHY Specifications. IEEE Std 802.11*. IEEE: New York, NY, 2007.
7. Thonet G, Allard-Jacquín P, Colle P. ZigBee - WiFi Coexistence. *Schneider Electric White Paper and Test Report*, April 2008.
8. Heinzelman W, Chandrakasan A, Balakrishnan H. Energy-efficient communication protocols for wireless microsensor networks. In *Proceedings of Hawaii International Conference on Systems Science*, Hunan, China, January 2000.
9. Zhang C, Liu J, Li H, Jiang X. Two-level routing protocol for mobile sensor network based on LEACH algorithm. In *International Conference on Intelligent Computing and Integrated Systems (ICISS)*, Guilin, China, October 2010; 950–953.
10. Arshad M, Saad NM, Kamel N, Armi N. Routing strategies in hierarchical cluster based mobile wireless sensor networks. In *International Conference on Electrical, Control and Computer Engineering (INECCE'11)*, Pahang, Malaysia, June 2011; 65–69.
11. Sun X, Coyle EJ. The effects of motion on applications in mobile ad-hoc sensor networks. In *IEEE 71st Vehicular Technology Conference (VTC'10)*, Taipei, Taiwan, May 2010.
12. Jianbo X, Jian G, Jing L, Xinlian Z. Mobile sink-based data gathering protocol. In *International Forum on Information Technology and Applications (IFITA)*, Kunming, China, July 2010; 427–430.
13. Oh S, Lee E, Park S, Jung J, Kim S. Communication scheme to support sink mobility in multi-hop clustered wireless sensor networks. In *24th IEEE International Conference on Advanced Information Networking and Applications (AINA'10)*, Perth, Australia, April 2010; 866–872.
14. Yu H, Guo M. An energy and delay aware data collection for mobile sink wireless sensor networks based on clusters. In *International Conference on Computer Application and System Modeling (ICCSM)*, Taiyuan, China, October 2010; volume 7, 536–540.
15. Joe I, Shin M. An energy-efficient mobile cluster-based approach for vehicular wireless sensor networks. In *6th International Conference on Networked Computing (INC)*, Gyeongju, Korea, May 2010.
16. Sarma H, Kar A, Mall R. Energy efficient and reliable routing for mobile wireless sensor networks. In *6th IEEE International Conference on Distributed Computing in Sensor Systems Workshops (DCOSSW)*, Santa Barbara, CA, June 2010.
17. Banerjee T, Agrawal DP. Increasing lifetime of wireless sensor networks using controllable mobile cluster heads. In *IEEE International Performance, Computing and Communications Conference (IPCCC 2008)*, Austin, Texas, December 2008; 77–84.
18. Deng S, Li J, Shen L. Mobility-based clustering protocol for wireless sensor networks with mobile nodes. *IET Wireless Sensor Systems* 2011; **1**(1): 39–47.
19. Jerew O, Liang W. Prolonging network lifetime through the use of mobile base station in wireless sensor networks. In *7th International Conference on Advances in Mobile Computing and Multimedia (MoMM '09)*, Kuala Lumpur, Malaysia, December 2009.
20. Khodashahi M, Tashtarian F, Moghaddam MY, Honary M. Optimal location for mobile sink in wireless sensor networks. In *IEEE Wireless Communications and Networking Conference (WCNC'10) (CD-ROM)*, Sydney, Australia, July 2010.
21. Ma M, Yang Y. Clustering and load balancing in hybrid sensor networks with mobile cluster heads. In *Proceedings of the 3rd International Conference on Quality of Service in Heterogeneous Wired/Wireless Networks (QShine'06)*, Waterloo, ON, August 2006.
22. Gao G, Miao G, Wang Q, Wang X. A mobile wireless sensor networks prediction algorithm based on clustering. In *International Conference on Educational and Network Technology (ICENT 2010)*, Qinhuaungdao, China, June 2010; 522–526.
23. Jaber S, Rahmani A, Khademzadeh A. Trusted data fusion by using cellular automata in wireless sensor networks. In *Proceedings of the 8th Annual Collaboration, Electronic Messaging, Anti-abuse and Spam Conference (CEAS '11)*, Perth, Australia, September 2011; 145–151.

24. Zhao M, Yang Y. A framework for mobile data gathering with load balanced clustering and MIMO uploading. In *Proceedings of IEEE INFOCOM 2011*, Shanghai, China, June 2011; 2759–2767.
25. Kim T, Jung S, Lee S. CMMP: clustering-based multi-channel MAC protocol in VANET. In *Second International Conference on Computer and Electrical Engineering (ICCEE '09)*, Dubai, UAE, December 2009; 380–383.
26. Zhang X, Wang H, Khokhar A. An energy-efficient MAC-layer retransmission algorithm for cluster-based sensor networks. In *IEEE International Networking and Communications Conference (INCC 2008)*, Lahore, Pakistan, May 2008; 67–72.
27. Zen K, Lenando H, Jambli MN. Load balancing based on nodes distribution in mobile sensor network. In *7th International Conference Information Technology in Asia (CITA'11)*, Sarawak, Malaysia, July 2011.
28. Lin C, Xue S, Yao L. Position calculating and path tracking of three dimensional location system based on different wave velocities. In *Proceedings of Eighth IEEE International Conference on Dependable, Automatic and Secure Computing (DASC'09)*, Chengdu, December 2009; 436–441.
29. Didi F, Feham M, Labiod H, Pujolle G. Dynamic admission control algorithm for WLANs 802.11. In *3rd International Conference on Information and Communication Technologies: From Theory to Applications (ICTTA '08)*, Damascus, Syria, April 2005.
30. Mišić J, Shafi S, Mišić VB. Maintaining reliability through activity management in a 802.15.4 sensor cluster. *IEEE Transactions on Vehicular Technology* 2006; **55**(3): 779–788.
31. *Artifex v.4.4.2*. RSoft Design Group, Inc.: San Jose, CA, 2003.
32. Vogt H. Efficient object identification with passive RFID tags. In *Proceedings of the First International Conference on Pervasive Computing (Pervasive '02)*, Zürich, Switzerland, 2002; 98–113.

AUTHORS' BIOGRAPHIES



Haleh Khojasteh received her BS degree in Electrical and Computer Engineering from Shahid Beheshti University, Tehran, Iran and her MS (2011) degree in Computer Science from Ryerson University. She is currently a PhD student in the Department of Computer Science at the Ryerson University. Her research interests are wireless sensor networks and mobile networks with emphasis on mathematical modeling and performance analysis.



Jelena Mišić received her PhD degree in Computer Engineering from University of Belgrade, Serbia, in 1993. She is currently a professor of Computer Science at Ryerson University, Toronto, Canada. Her research interests include wireless networks and security in wireless networks.



Vojislav B. Mišić received his PhD in Computer Science from University of Belgrade, Serbia, in 1993. He is a professor of Computer Science at Ryerson University in Toronto, Ontario, Canada. His research interests include performance evaluation of wireless networks and systems, and software engineering.